Surface & Coatings Technology 231 (2013) 428–432

Contents lists available at ScienceDirect

Surface & Coatings Technology

journal homepage: www.elsevier.com/locate/surfcoat

Zinc oxide thin-film transistors fabricated via low-temperature hydrothermal method

Jyh-Liang Wang [a,*], Po-Yu Yang [b], Miin-Horng Juang [c], Tsang-Yen Hsieh [a], Chuan-Chou Hwang [a], Chuan-Ping Juan [d], I-Che Lee [b]

[a] Department of Electronics Engineering, Ming Chi University of Technology, New Taipei 24301, Taiwan
[b] Department of Electronics Engineering and Institute of Electronics, National Chiao Tung University, Hsinchu 30010, Taiwan
[c] Department of Electronic Engineering, National Taiwan University of Science and Technology, Taipei 106, Taiwan
[d] Department of Electronics Engineering, St. John's University, New Taipei 25135, Taiwan

ARTICLE INFO

Available online 18 February 2012

Keywords:
Zinc oxide (ZnO)
Hydrothermal growth (HTG)
Thin-film transistors (TFTs)
Active-layer
Lateral growth

ABSTRACT

Transparent high-performance ZnO TFTs have been fabricated via low-temperature hydrothermal method. The dip of H_3PO_4 solution prior to the hydrothermal process can form the under-cut AZO seed layer and benefit for the control of ZnO growth. While the use of under-cut AZO seed layer with proper design of channel length, the lateral ZnO growth can be artificially controlled in the desired location to make a continuous active-layer and nearly single one vertical grain boundary cross to the current flow in the channel region. ZnO TFTs indicate the behavior of n-channel enhancement-mode devices. The optimum design of channel length (i.e. L = 10 μm) can provide enough space for the lateral growth of large ZnO grains with less channel defects and bring about the advanced device characteristics (i.e. the positive threshold voltage of 3.0 V, mobility of 9.03 $cm^2/V \cdot s$, on/off current ratio $>10^6$, gate leakage of <1 nA with less fluctuation, and extremely high drain current >500 μA).

1. Introduction

Zinc oxide (ZnO) has been investigated for various applications including ultraviolet photodetector [1], gas sensors [2], solar cells [3], light emitting diodes (LED) [4], and transparent electrodes [5] due to the properties of a direct energy wide-bandgap (i.e., ~3.37 eV), a large exciton binding energy (i.e., ~60 meV), good photoelectric and piezoelectric properties, and high optical transparency for visible light [6]. Recently, ZnO as an active channel layer has been investigated for transparent thin-film transistor (TFT) [7,8]. ZnO TFTs disclose not only the high transparency within the visible-light spectra but also the relatively high field effect mobility, less light sensitivity, and excellent chemical and thermal stability [9], indicating the potentials of ZnO-based thin-films applied in TFTs. However, the traditionally sputtered ZnO TFTs request expensive vacuum facilities and suffer degraded device characteristics owing to a large number of grain boundaries and many small grains of ZnO film formed at room temperature [10,11]. The grain boundaries produce potential wells that can trap and impede the movement of carriers and retard the transportation of carriers from grain to grain [12]. The existence of grain boundaries in the channel region of poly-ZnO TFT's has a dramatic influence on the electrical characteristics. For realizing the high-performance ZnO TFTs, it is essential not only to require larger ZnO grains but also to control the location, number, and direction of grain boundaries in ZnO active-layer. In this work, a simple hydrothermal method was considered for the ZnO thin-film growth because of the advantages of low-cost facility, capabilities of large-area and uniform fabrication, and environmental friendliness. A technique of nucleation at the selected region will be proposed, and the related device performances of ZnO TFTs are also addressed.

2. Experimental details

A commercial indium-tin-oxide (ITO) film sputtered on the glass substrate was used as the gate electrode with the thickness of 200 nm and resistivity of ~0.014 Ω-cm. The ITO/glass substrate was cut with the size of ~2 cm × 2 cm for device fabrication. After cleaning, a 200 nm-thick tetraethylorthosilicate silicon dioxide (TEOS-SiO_2) layer was deposited as gate dielectric by a plasma-enhanced chemical vapor deposition (PECVD) at 350 °C. Sputtered aluminum-doped ZnO (AZO), Ti, and Pt films were sequentially deposited at room temperature and patterned by lift-off process. The Pt (50 nm)/Ti (100 nm) films structure the electrodes of source/drain with the deposition parameters: DC process powers of 40 W/100 W, and deposition rates of ~0.1 Å/s/0.5 Å/s, correspondingly, under a fixed pressure of ~8 mTorr. The intermediate Ti film plays as an adhesion layer between Pt and AZO films. The AZO film was sputtered with an AZO ceramic target, RF process power of 150 W, deposition rate of ~0.5 Å/s, and

* Corresponding author at: 84 Gungjuan Rd., Taishan, Taipei 24301, Taiwan. Tel.: +886 2 29089899x4861; fax: +886 2 29085247.
E-mail address: joewang@mail.mcut.edu.tw (J.-L. Wang).

0257-8972/$ – see front matter © 2012 Elsevier B.V. All rights reserved.
doi:10.1016/j.surfcoat.2012.02.029

controlled pressure of ~4 mTorr. The function of AZO film is a seed layer for ZnO nucleation and growth during hydrothermal method [13]. Some of the samples were dipped in 0.001 M H_3PO_4 to under-cut the AZO seed layer, and the others were not. Then, each sample was immersed in the mixed hydrothermal solution to grow the lateral ZnO film. The growth solution was prepared by mixing with 0.25 M zinc nitrate hexahydrate ($Zn(NO_3)_2 \cdot 6H_2O$) with 0.25 M hexamethylenetetramine (HMTA) in deionized water at 85 °C. Subsequently, the samples were thoroughly rinsed with deionized water in order to eliminate the residual salts and dried in air at room temperature. As the reported investigation [14], the crystallinity of hydrothermal ZnO nanostructures can be evidently enhanced after 400 °C-oxygen ambient annealing. Therefore, all of the samples were annealed at 400 °C in oxygen ambience for 1 h. Some technologies of material analysis were applied to characterize the physical properties of hydrothermal ZnO films. The surface morphologies were observed by a field-emission scanning electron microscopy (FE-SEM, Hitachi S-4700I). The surface roughness of films was inspected by an atomic force microscope (AFM, Digital Instruments Nano-Scope III). The crystal structure of prepared devices was examined by X-ray diffraction (XRD) with a diffractometer (M18XHF, MAC Science) with the incident radiation of Cu Kα (i.e. $\lambda = 0.154$ nm). The optical emission properties were analyzed by photoluminescence (PL) spectra with He-Cd laser (i.e. $\lambda = 325$ nm) excitation. After ZnO TFT fabrication, an automatic measurement system that combines IBM PC/AT, semiconductor parameter analyzer (4156C, Agilent Technologies) and a probe station were used to measure the I–V characteristics.

3. Results and discussion

Fig. 1(a) gives the XRD pattern of hydrothermal ZnO films. The diffraction peaks of (100), (002), and (101) indicate that the ZnO film has hexagonal wurtzite-structure. The Pt (111) peak is related to the Pt film. Fig. 1(b) gives the PL emission spectra of hydrothermal ZnO film. The PL emission spectra can be distinguished as UV emission owing to the near band-edge emission (NBE) [15], and deep level emission (DLE) in the visible region due to the existence of structural defects [16,17]. Thus, the weak DLE and strong NBE intensities of hydrothermal ZnO film reflected the well crystal quality and few structural defects [16].

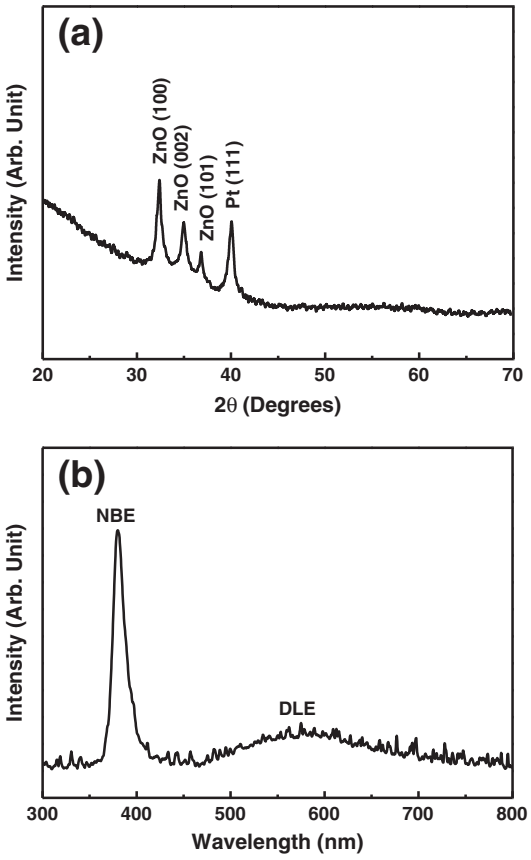

Fig. 1. (a) XRD diffraction pattern, and (b) room-temperature PL emission spectra of hydrothermal ZnO film.

As the prior study [13], hydrothermal ZnO grains can nucleate around the edges of the sputtered ZnO seed layer. Therefore, the region and distribution of AZO seed layer can affect the nucleation of hydrothermal ZnO grains. To investigate the control of hydrothermal ZnO nucleation at the selected region, some samples were dipped in H_3PO_4 solution to under-cut the AZO seed layer prior to the ZnO growth, and the others were not. The FE-SEM image for the samples dipped with H_3PO_4 solution is shown in Fig. 2(a), which confirms that the ZnO grain growth can not occur on the sputtered Pt/Ti electrodes. The ZnO grains grew from the edges of seed layer beneath the under layered Pt/Ti films. Near the Pt/Ti electrodes, a lot of small ZnO grains crowded and competed to grow. Then, the small ZnO grains merged and laterally extended toward the middle of the channel. The laterally hydrothermal growth can achieve a length of ~6 μm in the immersion duration of 5 h. On the contrary, Fig. 2(b) presents broken Pt/Ti electrodes for the samples without the dip of H_3PO_4 solution. The growth direction was not laterally restricted and the grains staggered. The growth rate is almost doubled (i.e. ~10 μm/5 h), compared to that of the samples dipped with H_3PO_4 solution. The rapid growth may bring huge stress among the

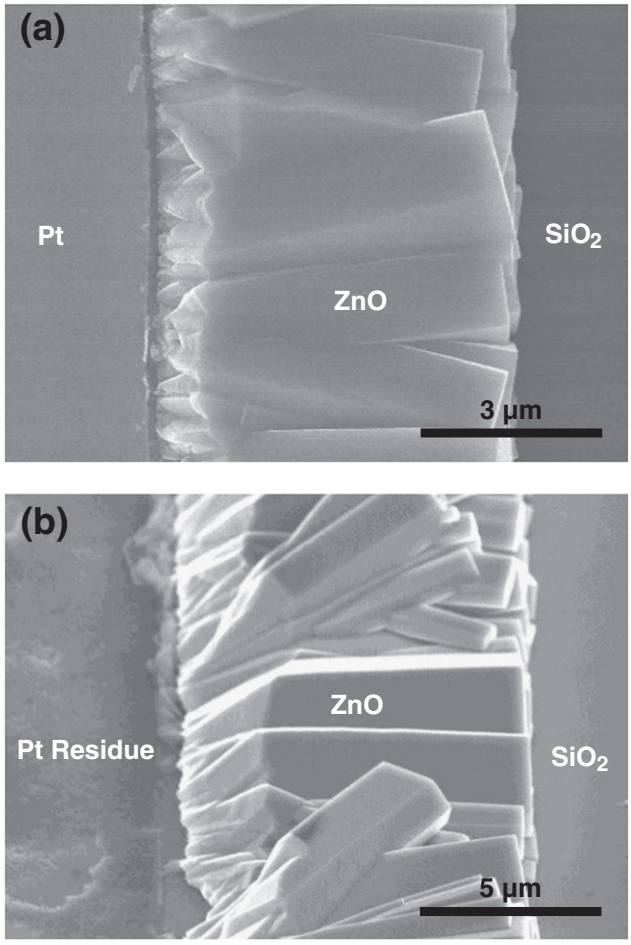

Fig. 2. FE-SEM images indicate the lateral growth of hydrothermal ZnO films (a) with, and (b) without the dip of H_3PO_4 solution. The immersion time was controlled as 5 h for hydrothermal growth.

hydrothermal ZnO grains and Pt/Ti electrodes, resulting in the broken Pt/Ti electrodes and the contact issue for electrical measurement. It recommends that the dip of H_3PO_4 solution prior to hydrothermal process can form under-cut AZO seed layer beneath Pt/Ti films and limit the growth direction and rate, which can be connected to the control of ZnO nucleation at the selected region. Thus, the dip of H_3PO_4 solution was adopted for the samples, addressed afterward.

Fig. 3 presents the top-view FE-SEM images to show the channel morphology of hydrothermal ZnO TFTs with different channel lengths. The immersion duration of hydrothermal ZnO growth was restricted as 3 h. The images of samples with the channel length (L) of 5 μm and 10 μm demonstrate similar channel morphology. The ZnO grain growth only existed between the sputtered Pt/Ti electrodes and no ZnO film is observed on the electrodes. The hydrothermally lateral growth started from the edges of AZO seed layer beneath the Pt/Ti electrodes, and extended toward the middle of the channel. The lateral grains grew from the opposite direction and collided at the middle of channel. However, the hydrothermal growth distance was limited and can not shape a continuous active-layer while the channel is too long (i.e. L = 25 μm).

Fig. 4(a) displays the AFM images for ZnO active-layer to perform the surface roughness of hydrothermal ZnO active-layer in channel region (while L = 10 μm). It indicates a rough surface. The ups and downs of surface interlace resemble laterally parallel valleys and dependent on the lateral growth of hydrothermal ZnO film. Moreover, Fig. 4(b) presents the cross-sectional FE-SEM image for the lateral ZnO growth in the channel region. The laterally grown ZnO grains impinged with each other and were artificially controlled to collide in the middle of the channel region above the gate oxide. The laterally collided ZnO grains result in only a single grain boundary perpendicular to the channel direction, which is consistent with the inspections of top-view FE-SEM and AFM.

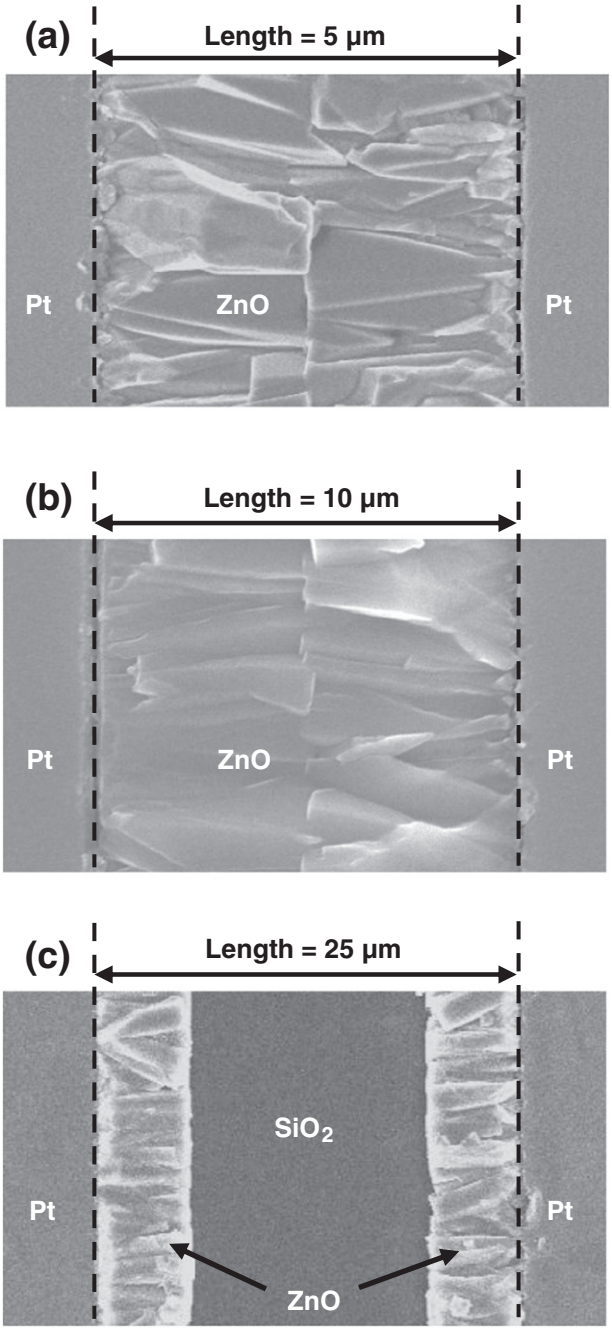

Fig. 3. Top-view FE-SEM images show the channel morphology of hydrothermal ZnO TFTs with the channel lengths (L) of (a) 5 μm, (b) 10 μm, and (c) 25 μm, accordingly. The immersion time was restricted as 3 h for hydrothermal growth.

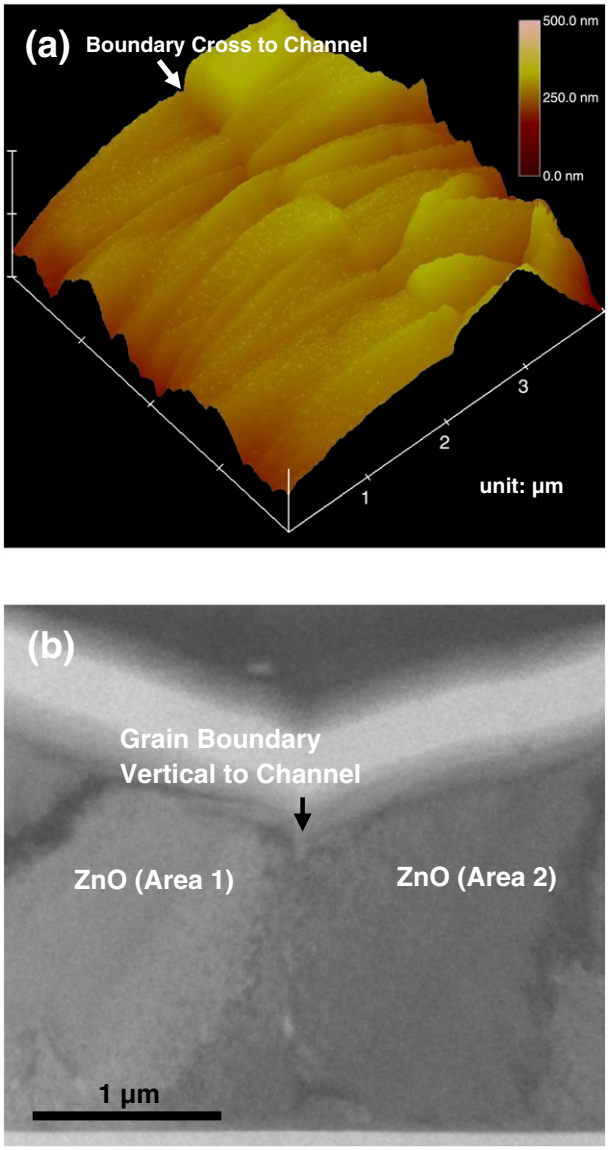

Fig. 4. (a) AFM image reveals the surface roughness of hydrothermal ZnO active-layer in channel region. (b) Cross-sectional FE-SEM image demonstrates that the lateral ZnO growth collided at the middle of channel. The channel length of the samples is designed as 10 μm.

The physical observations can be summarized as a schematic illustration for the lateral growth of hydrothermal ZnO active-layer, shown in Fig. 5. The ZnO grains grew from the edges of AZO seed layer beneath the under the Pt/Ti electrodes, and formed many small crowded ZnO grains near the electrodes. The small ZnO grains competed to grow and then merged to appear large grains which laterally extended toward the middle of the channel from opposite both sides. While the use of under-cut AZO seed layer with proper design of source/drain distance (channel length), the lateral ZnO growth can be artificially controlled in the desired location to make a continuous active-layer and the vertical grain boundary cross to the current flow in the channel region can be reduced to nearly single one. The localized potential barriers of grain boundaries could retard the transportation of carriers among grains [12]. The reduced vertical grain boundary (i.e. the nearly single one vertical grain boundary) in channel region is expected to make the improved device performance of hydrothermal ZnO TFTs.

Fig. 6 describes the drain current versus gate voltage (I_{DS} vs. V_{GS} and $I_{DS}^{1/2}$ vs. V_{GS}) of transfer characteristics and gate leakage current (I_{GS}) for the hydrothermal ZnO TFTs with the drain voltage (V_{DS}) of 20 V. The channel width (W) was fixed as 250 μm, and the channel length (L) was designed as 5 or 10 μm. The threshold voltage (V_{TH}) and field-effect mobility (μ_{FE}) were calculated with a line fitting of the square root of drain current versus gate voltage, defined by the drain current in saturation region [18]:

$$I_{DS,SAT} = \frac{W\mu_{FE}C_{OX}}{2L}(V_{GS}-V_{TH})^2 \quad (1)$$

where $I_{DS,SAT}$ is the saturated drain current, and C_{OX} is the capacitance per unit area of gate insulator, respectively. The V_{TH}, μ_{FE}, and on/off current ratio are extracted from Fig. 6(a) as 6.3 V, 3.89 $cm^2/V\cdot s$, and 1.3×10^6, respectively, for the ZnO TFTs with W/L = 250 μm/5 μm. On the contrast, Fig. 6(b) indicates the values of V_{TH}, μ_{FE}, and on/off current ratio as 3.0 V, 9.03 $cm^2/V\cdot s$, and 1.1×10^6, accordingly, for the ZnO TFTs with W/L = 250 μm/10 μm. ZnO TFTs require a positive gate voltage to turn-on, suggesting the behavior of n-channel enhancement-mode devices. The long-channel TFTs (i.e. L = 10 μm) exhibit the lower V_{TH} and higher μ_{FE} than short-channel devices (i.e. L = 5 μm), which violates the common experience and may be attributed to the laterally larger ZnO grains in the channel region of long-channel TFTs. The laterally larger ZnO grains suppose the fewer defects in the channel region, resulting in the easy turn-on (i.e. low V_{TH}) and profit on a carrier movement (i.e. high μ_{FE}). Furthermore, both the two W/L designs of TFTs expose the high on/off current ratio (over 6 orders) and low gate leakage current (~or <1 nA). The long-channel TFTs indicate the lower I_{GS} with less fluctuation, which suggests the stable device property.

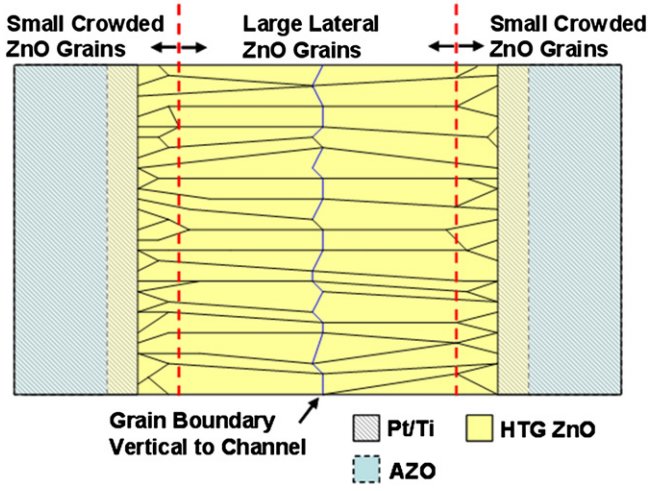

Fig. 5. Schematic illustration for the lateral growth of hydrothermal (HTG) ZnO active-layer.

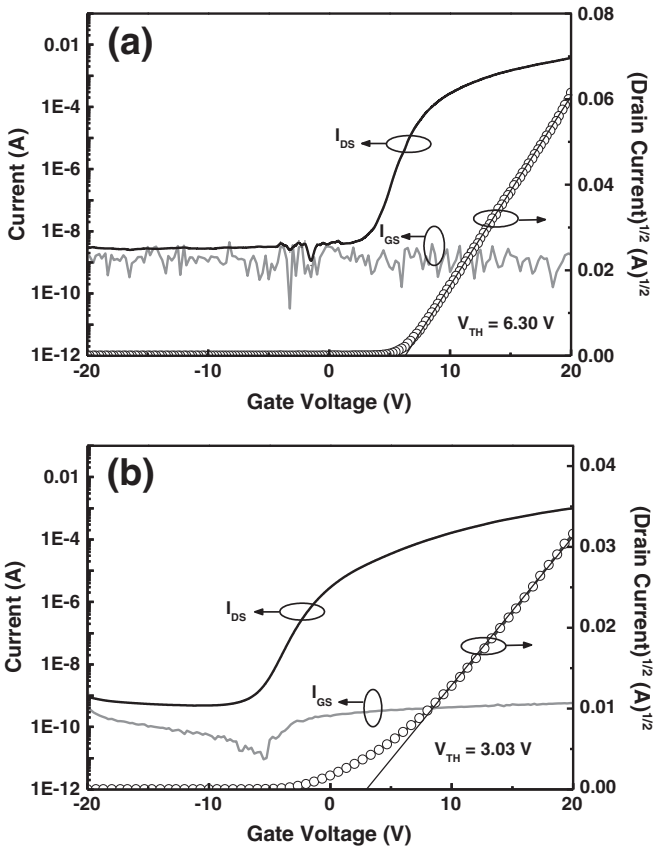

Fig. 6. Transfer characteristics (I_{DS}–V_{GS} and $I_{DS}^{1/2}$–V_{GS}) and gate leakage current (I_{GS}) of the hydrothermal ZnO TFTs with (a) W/L = 250 μm/5 μm, and (b) W/L = 250 μm/10 μm at the drain voltage (V_{DS}) of 20 V.

Fig. 7 demonstrates the drain current-drain voltage (I_{DS} vs. V_{DS}) of hydrothermal ZnO TFTs under V_{GS} = 0–20 V with the step of 5 V. The drain current of ZnO TFTs increased linearly with drain voltage at low values, and the saturation behavior was observed at high drain voltages due to the pinch-off effect by accumulation layer. In Fig. 7(a), the short-channel ZnO TFTs show the higher driving current than that of long-channel ZnO devices under the same bias conditions, which is associated with the higher lateral electrical field (i.e. V_{DS}/L) in the channel. The I_{DS} curves of short-channel ZnO TFTs tie together while the operation in the linear region. It discloses the current saturation at high gate voltages and the presence of current crowding at low gate voltages, which may be attributed to the extra defects owing to the more small crowded grains in the channel. Contrarily, the samples with L = 10 μm express the typical I_{DS}–V_{DS} curves. An extremely high I_{DS} of 500 μA could be achieved with V_{DS} below 14 V (while V_{GS} = 20 V). Consequently, the optimum design of channel length (i.e. L = 10 μm) can provide the enough space for the laterally hydrothermal growth of larger ZnO grains with less channel defects and bring about the advanced device characteristics (i.e. the lower positive V_{TH}, higher μ_{FE}, high on/off current ratio, lower I_{GS} with less fluctuation, and high I_{DS}).

4. Conclusion

The transparent zinc oxide (ZnO) TFTs have been fabricated via hydrothermal method on the glass substrates at 85 °C. The hydrothermal ZnO films indicated the hexagonal wurtzite-structure with well crystal quality. The dip of H_3PO_4 solution prior to the hydrothermal

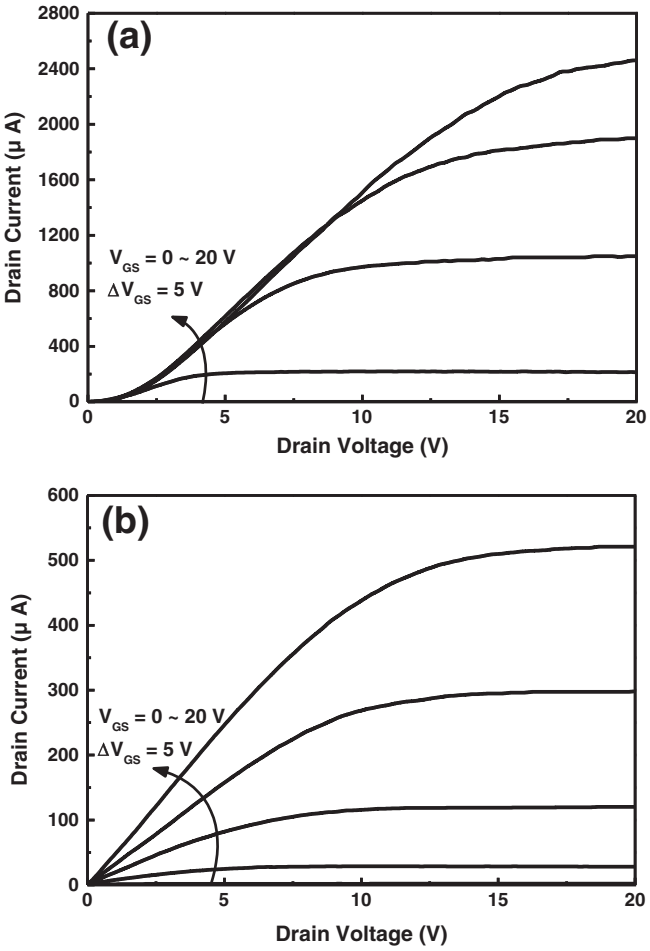

Fig. 7. Output characteristics (I_{DS}–V_{DS}) of the hydrothermal ZnO TFTs with (a) W/L = 250 μm/5 μm, and (b) W/L = 250 μm/10 μm under the gate voltage (V_{GS}) of 0–20 V with the step of 5 V.

process can form the under-cut aluminum-doped ZnO (AZO) seed layer, which limited the nucleation of ZnO grains at the selected region. The growth of ZnO films started from the edges of AZO seed layer beneath the Pt/Ti films, and laterally extended toward the middle of channel from the opposite directions. Many small crowded ZnO grains appeared near the Pt/Ti electrodes, and then merged to form large lateral grains. While the use of under-cut AZO seed layer with proper design of channel length, the lateral ZnO growth can be artificially controlled in the desired location to make a continuous active-layer and nearly single one vertical grain boundary cross to the current flow in the channel region. ZnO TFTs require positive gate voltage to turn-on, suggesting the behavior of n-channel enhancement-mode devices. The optimum design of channel length (i.e. L = 10 μm) can provide enough space for the laterally hydrothermal growth of larger ZnO grains with less channel defects and bring about the advanced device characteristics (i.e. the low positive threshold voltage of 3.0 V, high mobility of 9.03 $cm^2/V \cdot s$, high on/off current ratio $>10^6$, low gate leakage of <1 nA with less fluctuation, and high drain current >500 μA).

Acknowledgments

Thanks are due to the Center for Thin Film Technologies and Applications (CTFTA) in Ming Chi University of Technology, the Nano Facility Center (NFC) in National Chiao Tung University, and the National Nano Device Laboratory (NDL) for the technical supports.

References

[1] H.S. Bae, S. Im, Thin Solid Films 469 (2004) 75.
[2] S.P.S. Arya, O.N. Srivastava, Cryst. Res. Technol. 23 (1988) 669.
[3] C. Lee, K. Lim, J. Song, Sol. Energy Mater. Sol. Cells 43 (1996) 37.
[4] S.K. Hazra, S. Basu, Solid State Electron. 49 (2005) 1158.
[5] V. Assuncao, E. Fortunato, A. Marques, H. Aguas, I. Ferreira, M.E.V. Coata, R. Martins, Thin Solid Films 427 (2003) 401.
[6] S.J. Lim, S. Kwon, H. Kim, Thin Solid Films 516 (2008) 1523.
[7] C.J. Kao, Y.W. Kwon, Y.W. Heo, D.P. Norton, S.J. Pearton, F. Ren, G.C. Chi, J. Vac. Sci. Technol. B 23 (2005) 1024.
[8] P.F. Carcia, R.S. McLean, M.H. Reilly, Appl. Phys. Lett. 88 (2006) 123509.
[9] C.Y. Tsay, K.S. Fan, S.H. Chen, C.H. Tsai, J. Alloys Compd. 495 (2010) 126.
[10] Y. Kwon, Y. Li, Y.W. Heo, M. Jones, P.H. Holloway, D.P. Norton, Z.V. Park, S. Li, Appl. Phys. Lett. 84 (2004) 2685.
[11] R.B.M. Cross, M.M. De Souza, S.C. Deane, N.D. Young, IEEE Trans. Electron Devices 55 (2008) 1109.
[12] F.M. Hossain, J. Nishii, S. Takagi, A. Ohtomo, T. Fukumura, H. Fujioka, H. Ohno, H. Koinuma, M. Kawasaki, J. Appl. Phys. 94 (2003) 7777.
[13] P.Y. Yang, J.L. Wang, W.C. Tsai, S.J. Wang, J.C. Lin, I-Che Lee, C.T. Chang, H.C. Cheng, Thin Solid Films 518 (2010) 7328.
[14] P.Y. Yang, J.L. Wang, W.C. Tsai, S.J. Wang, J.C. Lin, I.C. Lee, C.T. Chang, H.C. Cheng, J. Nanosci. Nanotechnol. 11 (2011) 5737.
[15] Y.C. Kong, D.P. Yu, B. Zhang, W. Fang, S.Q. Feng, Appl. Phys. Lett. 78 (2001) 407.
[16] R.C. Wang, C.P. Liu, J.L. Huang, S.J. Chen, Appl. Phys. Lett. 88 (2006) 023111.
[17] Q. Wan, T.H. Wang, J.C. Zhao, Appl. Phys. Lett. 87 (2005) 083105.
[18] H.H. Hsieh, C.C. Wu, Appl. Phys. Lett. 89 (2006) 041109.